Design and Synthesis of a Transition Metal Responsive Semisynthetic Myoglobin-Bearing Iminodiacetic Acid Moiety

Itaru Hamachi,* Tomoaki Matsugi, Kengo Wakigawa, and Seiji Shinkai

Department of Chemistry & Biochemistry, Graduate School of Engineering, Kyushu University, Hakozaki, Fukuoka 812-8581, Japan

Received December 12, 1996

Iminodiacetic acid appended myoglobins (IDA*n*-Mb, $n = 1, 2$) were synthesized by conventional reconstitution of chemically modified hemes with apomyoglobin. The metal responsive property of the obtained IDA*n*-Mb was studied by metal ion titration, pH titration, circular dichroism (CD) and ^{1}H NMR spectroscopies, and reduction with ascorbate. IDA*n*-Mb quantitatively bound various transition metal cations (Co^{2+}, Ni^{2+}, Zn^{2+}, Cd^{2+}, and Cu^{2+}) but not Mg^{2+}. The binding stoichiometry of IDA2-Mb was 1:1 for Co^{2+}, Ni^{2+}, Zn^{2+}, and Cd^{2+} and 1:2 for Cu^{2+}, whereas the stoichiometry of 1:1 was shown for IDA1-Mb to all transition metals (Co^{2+}, Ni^{2+}, Zn^{2+}, Cd^{2+}, and Cu^{2+}). The acidic pK_a shift of the H_2O coordinated to the heme iron(III) was clearly observed upon the binding of transition metals, suggesting the microenvironmental change of the heme crevice. This was supported by the CD and ^{1}H NMR spectra of IDA*n*-Mb. The transition metal induced structural changes of IDA*n*-Mb were reflected in their redox behavior, i.e., the reduction rate of IDA2-Mb by ascorbate was enhanced 8-fold upon the Co^{2+} binding. The rate showed a good linear relationship with the shifted pK_a of the axial H_2O, indicating that the transition metal binding directly affects the electron acceptability of IDA*n*-Mb. These results demonstrated that iminodiacetic acid moieties can play a crucial role as a reporter molecule for design of a transition metal responsive semisynthetic protein.

Introduction

Hemoproteins in natural systems are known to perform diverse functions such as electron transport (cytochromes), O_2 transport or storage (hemoglobin or myoglobin), and substrate oxidation (oxygenase or peroxidase).[1] Accumulated research from the past several decades shows that heme−apoprotein interactions including the sort of the axial ligand or the microenvironment of the heme active site rigidly control the molecular functions of the hemoproteins. These results elicit an interesting idea that the artificial regulation of the heme−apoprotein interactions can switch the hemoprotein activity.[2] We are now interested in molecular engineering for hemoproteins, not only to elucidate their structure−function relationships in chemical aspects but also to create novel biocatalysts based on the templates of native proteins.[3] The well-defined framework of some hemoproteins is one of the ideal models to evaluate the structure−function relationship of the engineered proteins in the molecular term. We recently found that the incorporation of phenylboronic acid capable of binding sugars can confer a sugar responsive property on the engineered myoglobin (Mb).[4] This example suggested that rational introduction of artificial receptors into naturally occurring proteins and enzymes may become a novel strategy for the development of stimuli responsive semiartificial proteins. To generalize this concept, we are now attempting to expand the sort of artificial receptors which are promising for the function modulation of native proteins. Here we describe that the active-site directed modification of Mb with iminodiacetic acid group can facilitate an electron-transfer reaction from ascorbate to Mb with response to the transition metal binding. The metal responsive properties in the structure and the function of the iminodiacetic acid appended myoglobins are discussed in detail.

Results

Design of Iminodiacetic Acid Pendant Myoglobins. As a metal-binding site, iminodiacetic acid is selected because of its high affinity to various transition metals ($K_{ass} = 10^6 \sim 10^8$ M^{-1} for transition metals).[5] Its low molecular weight and high water solubility are expected to be helpful for the modification of protein surfaces without denaturation. Iminodiacetic acid appended hemes **1** and **2** (Chart 1) were synthesized as shown in Scheme 1. Protoporphyrin IX (PPIX) was amidated with *N*,*N*-di(ethoxycarbonylmethyl)ethylenediamine, followed by iron insertion and hydrolysis to afford the heme **2**. According to the similar manner, the heme **1** was prepared from PPIX monoethyl ester as a starting material rather than from PPIX.

* E-mail: itarutcm@mbox.nc.kyushu-u.ac.jp.

(1) Yonetani, T. In *The Enzymes*; Boyer, P. D., Ed.; Academic Press: Orlando, FL, 1976; Vol. 13, pp 345.
(2) (a) Lloyd, E.; Hildebrand, D. P.; Tu, K. M.; Mauk, A. G. *J. Am. Chem. Soc.* **1995**, *117*, 6434. (b) Huang, X.; Boxer, S. G. *Nat. Struct. Biol.* **1994**, *1*, 226. (c) Sligar, S. G.; Egeberg, K. D. *J. Am. Chem. Soc.* **1987**, *109*, 7896. (d) Kamiya, N.; Shiro, Y.; Iwata, T.; Iizuka, T.; Iwasaki, H. *J. Am. Chem. Soc.* **1991**, *113*, 1826.
(3) (a) Hamachi, I.; Tanaka, S.; Shinkai, S. *J. Am. Chem. Soc.* **1993**, *115*, 10458. (b) Hamachi, I.; Nakamura, K.; Fujita, A.; Kunitake, T. *J. Am. Chem. Soc.* **1993**, *115*, 4966. (c) Hamachi, I.; Tanaka, S.; Shinkai, S. *Chem. Lett.* **1993**, 1417. (d) Hamachi, I.; Higuchi, S.; Nakamura, K.; Fujimura, H. Kunitake, T. *Chem. Lett.* **1993**, 1175. (e) Hamachi, I.; Nomoto, K.; Tanaka, S.; Tajiri, Y.; Shinkai, S. *Chem. Lett.* **1994**, 1139. (f) Hamachi, I.; Matsugi, T.; Tanaka, S.; Shinkai, S. *Bull. Chem. Soc. Jpn.* **1996**, *69*, 1657.
(4) (a) Hamachi, I.; Tajiri, Y.; Shinkai, S. *J. Am. Chem. Soc.* **1994**, *116*, 7437. (b) Hamachi, I.; Tajiri, Y.; Murakami, H.; Shinkai, S. *Chem. Lett.* **1994**, 575. (c) Hamachi, I.; Nagase, T.; Tajiri, Y.; Shinkai, S. *J. Chem. Soc., Chem. Commun.* **1996**, 2205.
(5) Martel, A. E.; Smith, R. M. *Crystal Stability Constants*; Plenum Press: New York, 1989; Vol. 1, pp 116−119.

S0020-1669(96)01474-7 CCC: $15.00
Published on Web 03/12/1998

Scheme 1. Reaction Scheme of IDA1- and IDA2-Heme[a]

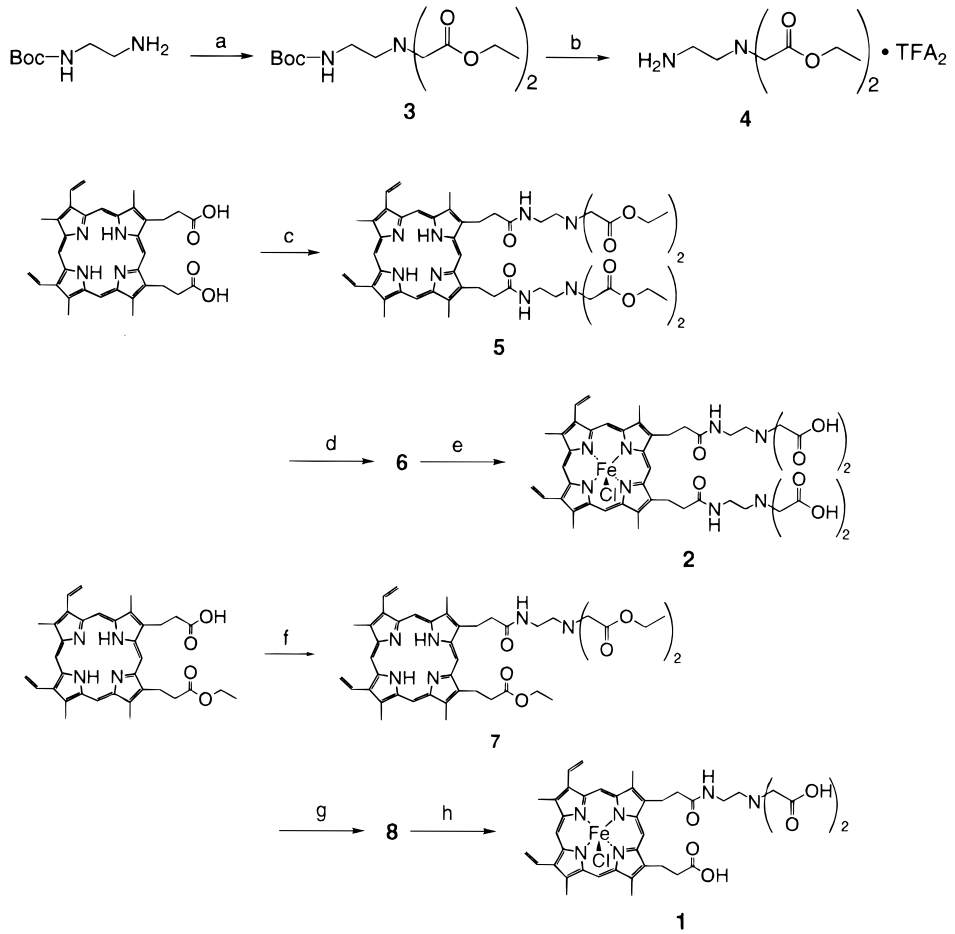

[a] (a) $BrCH_2CO_2Et$, $NaHCO_3$, DMF; (b) TFA, CH_2Cl_2; (c) **4**, BOP, DIEA, THF/DMF; (d) $FeCl_2$, DMF; (e) NaOH, MeOH, H_2O; (f) **4**, BOP, DIEA, THF/DMF; (g) $FeCl_2$, DMF; (h) NaOHaq, MeOH/H_2O.

Chart 1

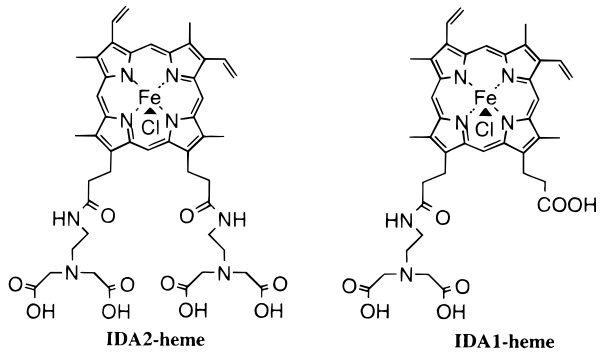

Incorporation of the heme **1** or **2** into apo-Mb was conducted by a slightly modified cofactor-reconstitution method,[6] to afford iminodiacetic acid appended myoglobins (IDA1-Mb and IDA2-Mb, respectively) with almost quantitative yield (95% for **1** and 90% for **2**). Ligand exchange reactions and redox reactions proved that IDA*n*-Mbs ($n = 1, 2$) are almost identical to native Mb in their active-site structure [UV−visible spectral data of these Mb derivatives are as follows: aqua-met native-Mb, max, 409, 505, and 633 nm; azide-met native-Mb, max, 422, 542, and 576 nm; fluoro-met native-Mb, max, 408, 546, and 606 nm; deoxy (Fe^{II})-native-Mb, max, 435, 560 nm; oxy-(O_2-complex) native-Mb, max, 418, 540, and 579 nm; aqua-met IDA2-Mb, max, 408, 502, and 630 nm; azide-met IDA2-Mb, max, 419, 542, and 575 nm; fluoro-met IDA2-Mb, max, 406 and 606 nm; deoxy (Fe^{II})-IDA2-Mb, max, 432 and 557 nm; oxy-(O_2-complex) IDA2-Mb, max, 413, 542 and 579 nm; aqua-met IDA1-Mb, max, 408, 498, and 629 nm; azide-met IDA1-Mb, max, 420, 539, and 575 nm; fluoro-met IDA1-Mb, max, 406 and 607 nm; deoxy-(Fe^{II})-IDA1-Mb, max, 431 and 558 nm; oxy-(O_2-complex)-IDA1-Mb, max, 413, 542, and 576 nm]. The ratio of the Soret absorbance (408 nm) to the protein absorbance (280 nm) is 5.2 and 5.1 for IDA1-Mb and IDA2-Mb, respectively. These values are greater than that of native Mb, indicating that IDA*n*-Mbs are pure enough for the subsequent experiments.[7]

Binding of Transition Metals to IDA*n*-Mbs. When various transition metal cations were added to the aqueous solution containing IDA*n*-Mbs, we observed the UV−visible spectral changes. Figure 1a shows a typical spectral change of IDA2-Mb by the addition of Co(II) cation. Increasing the amount of Co^{2+} lessens the absorbance of both the Soret band at 408 nm and the Q bands at 505 and 630 nm and simultaneously intensifies two Q bands at 540 and 580 nm with isosbestic points at 492, 525, and 628 nm. These changes depend linearly on the concentration of Co^{2+} and level off at 1 equiv of Co^{2+} addition (Figure 2b), indicating that a 1:1 complex between IDA2-Mb and Co^{2+} forms predominantly in the present condi-

(6) (a) Asakura, T. In *Methods in Enzymology*; Fleischer, S., Packer, L., Eds.; Academic Press: New York, 1978; Part C, p 446. (b) Teals, F. W. *J. Biochim. Biophys. Acta* **1959**, *35*, 543.

(7) Tamura, M.; Asakura, T.; Yonetani, T. *Biochim. Biophys. Acta* **1973**, *295*, 467.

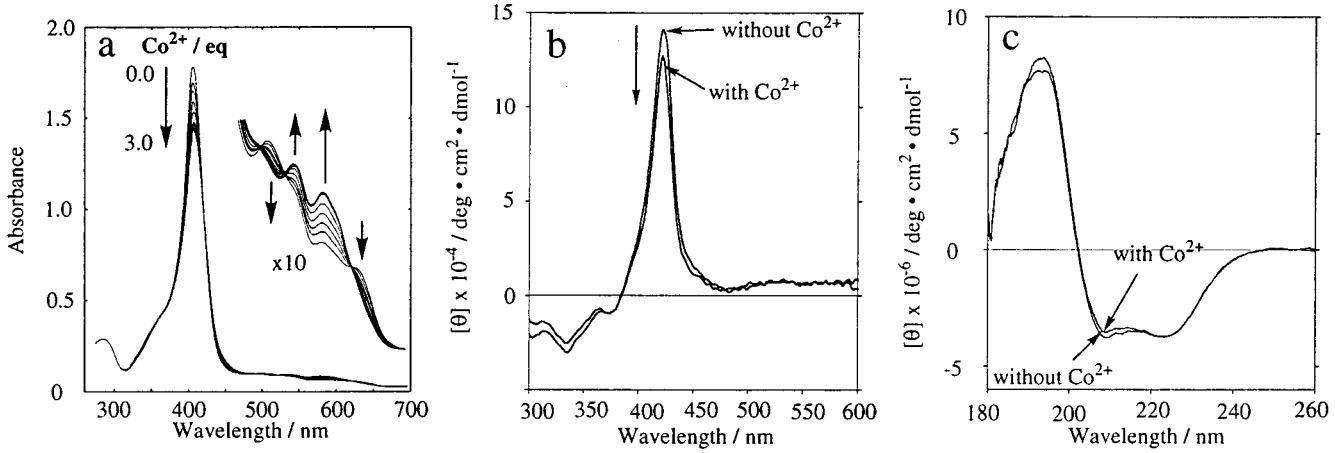

Figure 1. (a) UV−visible spectral change of IDA2-Mb upon addition of $CoCl_2$:IDA2-Mb, 13.7 μM in phosphate buffer (50 mM, pH 8.0) at 25 °C. (b) Visible and (c) UV regions of CD spectral change of IDA2-Mb by the addition of $CoCl_2$ (1 equiv):IDA2-Mb, 13.7 μM, KCN, 500 μM in phosphate buffer (50 mM, pH 7.0) at 25 °C.

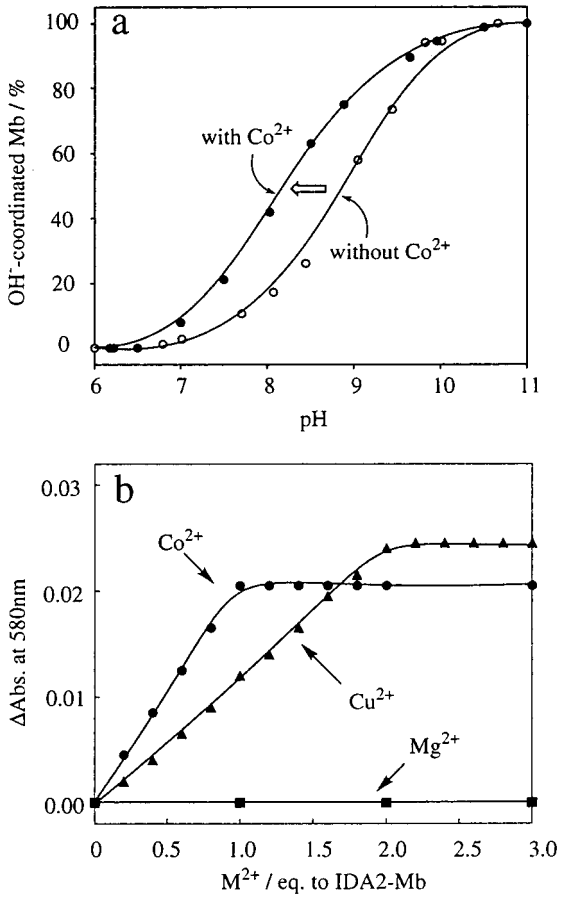

Figure 2. (a) Typical pH titration curves of IDA2-Mb monitored by UV−visible spectroscopy in the absence of and the presence of $CoCl_2$ (1 equiv). (b) Titration curves of the metal-induced absorbance change (580 nm).

tions. Similar spectral changes of IDA2-Mb take place for the other metal cations (Ni^{2+}, Zn^{2+}, and Cd^{2+}). For the Cu(II) cation, on the other hand, the spectral changes are saturated at a 1:2 ratio of IDA2-Mb to Cu^{2+}. This indicates the quantitative formation of a 1:2 complex (IDA2-Mb:Cu^{2+}) (see also Figure 2b). In the case of IDA1-Mb, the titration curves show typical saturation behavior at a 1:1 ratio (metal:IDA1-Mb) for all transition metals (Co^{2+}, Ni^{2+}, Zn^{2+}, Cd^{2+}, and Cu^{2+}; data not shown). Mg^{2+} never affects the UV−visible spectra of IDA1- and IDA2-Mb (Figure 2b).[8]

Table 1. pK_a Values of IDA2- and IDA1-Mb in the Presence of Several Metal Cations

	pK_a		
metal cation	IDA2-Mb	IDA1-Mb	native-Mb
none	8.9	9.0	9.0
Co^{2+} (1 equiv)	8.2	8.5	9.0
Ni^{2+} (1 equiv)	8.2	8.5	9.0
Cu^{2+} (1 equiv)	8.5	8.1	9.0
Cu^{2+} (2 equiv)	8.0		9.0
Zn^{2+} (1 equiv)	8.2	8.5	9.0
Cd^{2+} (1 equiv)	8.2	8.4	9.0
Mg^{2+} (5 equiv)	8.9	9.0	9.0

Transition Metals Induced pK_a Shift of the Coordinated H_2O. According to the literature, the absorbances at 505 and 630 nm that were lessened upon addition of transition metals are assigned to the absorption maxima due to a H_2O-coordinated Mb, and the intensified absorbances at 540 and 580 nm are due to a hydroxide-coordinated Mb.[9] The above-mentioned spectral changes (Figure 1a) induced by transition metals therefore suggest the acidic shift of pK_a of the H_2O coordinated to the heme iron(III). Careful pH titration experiments in the presence and the absence of metal ions clearly demonstrate the metal-induced pK_a shift for both IDA2-Mb and IDA1-Mb. Typical pH titration plots monitored by absorption spectroscopy (IDA2-Mb with and without Co^{2+}) are displayed in Figure 2a. It is apparent that the pK_a value is shifted from 8.9 to 8.2 by addition of 1 equiv of Co^{2+}.[10] Table 1 summarizes all the pK_a values of IDA*n*-Mb in the presence of various divalent metal cations. We should note the following important points: (i) pK_a values for IDA1- and IDA2-Mb in the absence of metals are almost comparable to that of native Mb;[11] (ii) addition of transition metals (Co^{2+}, Ni^{2+}, Cu^{2+}, Zn^{2+}, and Cd^{2+}) causes the acidic pK_a shift for both IDA2-Mb and IDA1-Mb;[12] (iii) the pK_a shift

(8) It was reported that the stability constant of iminodiacetic acid for Mg^{2+} is $10^{2.98}$ M^{-1}, which is remarkably smaller than that for other transition metals (10^5−10^7 M^{-1}).

(9) (a) Antonini, E.; Brunori, M. *Hemoglobin and Myoglobin in Their Reactions with Ligands*; North-Holland Publishing Co.: Amsterdam, 1971. (b) Brunori, M.; Amiconi, G.; Antonini, E.; Wyman, J.; Zito, R.; Rossi Fanelli, A. *Biochim. Biophys. Acta* **1968**, *154*, 315.

(10) Curves of the pH titration of IDA*n*-heme incorporated in Triton X-100 micelle instead of apo-Mb did not change by addition of any transition metals.

(11) This indicates that iminodiacetic acid modification scarcely disturbs the Mb active site, which may be explained by the net anionic charge of iminodiacetic acid moiety and the less bulkiness, like the native propionate ends.

by metal cations is generally greater for IDA2-Mb than that for IDA1-Mb; (vi) the metal-induced pK_a shift is saturated at the binding stoichiometry of IDA*n*-Mb to metals which is mentioned above; (v) Mg^{2+} does not have any effect on the pK_a of IDA*n*-Mb.

The considerable pK_a shift induced by transition metals may imply that the microenvironment of the active site (i.e., heme crevice) alters by the metal binding at the IDA moiety. Figure 1b,c shows circular dichroism (CD) spectra of IDA2-Mb in the absence and the presence of Co^{2+} cation.[13] The induced CD peak of the heme (a positive Cotton effect at 408 nm) is clearly lessened by 10% in its intensity by the addition of Co^{2+} (1 equiv), whereas the α-helix region (two negative peaks at 220 and 208 nm and a positive peak at 190 nm) scarcely changes. For the other transition metals, IDA2-Mb shows the CD spectral changes similar to that for Co^{2+}. Mg^{2+} is not effective again. It is clear that the transition metal binding at the IDA2 site perturbs the active-site microenvironment more efficiently rather than the whole myoglobin structure. The similar but less distinguished CD changes of IDA1-Mb are induced by the transition metals.

^{1}H NMR spectra of IDA2-Mb in the absence and presence of Co^{2+} support these results. We observed the metal-induced chemical shift changes of the amino acid residues of Mb located in the proximity of the heme center: e.g., Phe (CD1); 16.8−16.6 ppm, Val (E10); −1.65 to −1.55 ppm, Leu (G5); −1.40 to −1.38; Ile (FG5); −3.10 to −3.05 and −3.50 to −3.46.[14] The upfield shift of the *para*-proton of Phe (CD1) implies that the paramagnetic shift due to iron(III) becomes small upon Co^{2+} binding. Similarly, the shift of Val (E10), Leu (G5), and Ile (FG5) suggests that the shielding effect due to the heme ring becomes weak. Such spectral observations consistently show that the heme−apomyoglobin interactions loosen upon Co^{2+} binding. No spectral changes in CD or in ^{1}H NMR occurred by the metal addition in native Mb.

Transition Metals Facilitated Reduction of IDA*n*-Mbs by Ascorbate. The transition metal induced structural changes of the active site of IDA*n*-Mbs were reflected in their redox properties. The reduction of met-IDA*n*-Mb (Fe(III) state) by ascorbate gives deoxy-Mb (Fe(II) state) which is rapidly oxygenated under aerobic conditions to form oxy-Mb (O_2-bound Mb).[15] This process can be spectrophotometrically monitored as shown in Figure 3. Obviously, the reduction rate of IDA2-Mb is accelerated 8-fold upon addition of Co(II) cation. Such enhancement is linearly dependent on the Co^{2+} concentration and is saturated at a 1:1 ratio of Co(II) to IDA2-Mb (inset of Figure 3). This saturation kinetics is in good agreement with the behavior of the metal-induced UV−visible changes. It is clear that the Co(II) binding directly affects the electron-transfer reaction. We measured the initial rates (V_{init}) for IDA2-Mb and IDA1-Mb in the presence and absence of various divalent metal cations. Generally, IDA2-Mb displays the greater rate enhancement by the addition of transition metals (Co^{2+}, Ni^{2+}, Cu^{2+}, Zn^{2+}, and Cd^{2+}) in this reduction, relative to IDA1-Mb.

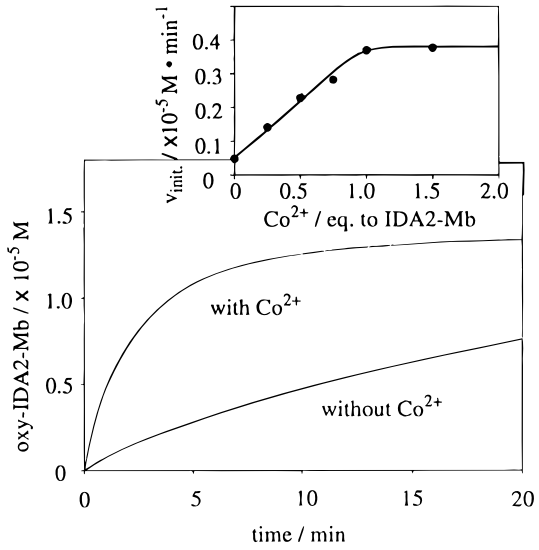

Figure 3. Time course of the reduction of IDA2-Mb by ascorbate (0.2 mM) in the presence and the absence of $CoCl_2$ (1 equiv). Inset: Dependence of the initial reduction rate of IDA2-Mb on $CoCl_2$ concentration: IDA2-Mb, 13.7 μM; KCN, 500 μM in phosphate buffer (50 mM, pH 7.0) at 25 °C.

The redox potentials ($E_{1/2}$) of IDA*n*-Mb were determined by spectroelectrochemistry using methylene blue (MB) as a mediator. The $E_{1/2}$ value of IDA2-Mb was 78 ± 10 mV (vs NHE) in the absence of metal cations, which is almost comparable value to that of native Mb. The addition of Co^{2+} (1 equiv) to IDA2-Mb scarcely caused any $E_{1/2}$ shift (69 ± 10 mV vs NHE). The $E_{1/2}$ in the presence of other transition metals (Ni^{2+}, Zn^{2+}, or Cd^{2+}) was also in the same range (78 ± 10 mV vs NHE). IDA1-Mb showed similar behavior for $E_{1/2}$ (63 ± 10 mV vs NHE in the absence of metals and 64 ± 10 mV vs NHE in the presence of Co^{2+}, Ni^{2+}, Zn^{2+}, or Cd^{2+}).

Discussion

UV−visible titration of IDA2-Mb with Co^{2+} clearly shows the generation of a stable complex having a 1:1 stoichiometry (Co^{2+}:IDA2-Mb). Because iminodiacetic acid (IDA) is a tridentate ligand, this ratio suggests that two IDA ligands in one Mb cooperatively work to form a hexagonal $Co(IDA)_2$ complex. Other transition metals such as Zn^{2+}, Ni^{2+}, and Cd^{2+} also show a 1:1 stoichiometry, indicating the formation of the similar complexes. In contrast, Cu^{2+} forms a 2:1 complex. It is probable that Cu^{2+} prefers a square-planar complex with IDA, so that 2 mol of the $Cu(IDA)_1$ complex are generated predominantly.

Complexation of IDA sites with transition metals is considered to cause breakage of electrostatic and hydrogen bonding interactions between IDA ends (carboxylic acid) and amino acid residues of the apo-Mb skeleton.[16] Conceivably, the weakening of the heme−apomyoglobin interactions as probed by the CD spectroscopy induces a considerable pK_a shift of the coordinated H_2O in the Mb active site. In fact, an acidic pK_a shift was already reported for a reconstituted Mb with a heme bearing

(12) The pK_a values are determined under the condition where more than 99% of IDA*n*-Mb's bind the corresponding transition metals.

(13) In CD experiments, we used the CN^--bound IDA*n*-Mb's in order to avoid the metal-induced UV−visible spectral change. It was confirmed that the CN^--bound IDA*n*-Mb's do not show any UV−visible change upon addition of metal cations.

(14) (a) Emerson, S. D.; La Mar, G. N. *Biochemistry* **1990**, *29*, 1556. (b) Emerson, S. D.; La Mar, G. N. *Biochemistry* **1990**, *29*, 1545. (c) Emerson, S. D.; Lecomte, G. N.; La Mar, G. N. *J. Am. Chem. Soc.* **1988**, *110*, 4176. Chemical shifts for Phe (CD1) and Val (E10) located in the distal side of the heme pocket slightly changed by replacement of protohemin to IDA2-heme (Phe (CD1), 17.2−16.8 ppm; and Val (E10), −1.95 to −1.65 ppm). However, pK_a values without metals, CD spectra, the stability of oxy-Mb, and the redox potentials suggest that the distal pocket is not significantly perturbed by the heme modification with IDA*n*.

(15) The dioxygen complex of IDA*n*-Mb was slowly autoxidized to met form. The autoxidation rate constants (k_{ox}) of oxy-IDA*n*-Mb were in the range of 0.2−0.4 h^{-1}, which are almost comparable to native Mb.[24] The values were slightly affected upon metal binding (0.1−0.2 h^{-1}).

(16) Evans, S. V.; Brayer, G. D. *J. Mol. Biol.* **1990**, *213*, 885.

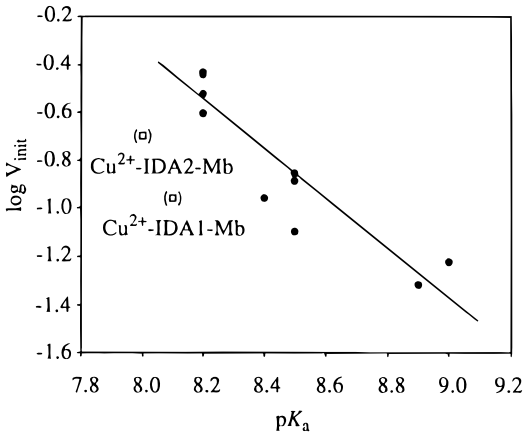

Figure 4. pK_a−initial rate profile of IDA*n*-Mb.

two propionate masked by methyl esters (the pK_a shifted from 9.0 (native) to 7.5),[17] due to the structural disturbance raised by the loss of the electrostatic interactions as well as by the steric repulsions between the heme side chains and peptide side chains. The above explanation is strongly supported by the result of the transition metals responsive behavior of IDA1-Mb. One propionate anion remains free to interact with apo-Mb unlike IDA2-Mb, even when a divalent metal is bound. Therefore, the heme−apomyoglobin interactions of IDA1-Mb do not become weaker upon the metal binding, rather than those for IDA2-Mb. This is consistent with the less acidic pK_a shift for the metal-bound IDA1-Mb than IDA2-Mb. Cu^{2+} is regarded as an exception again.

The pK_a reduction rate (log V_{init}) profile in Figure 4 shows that the reduction rate of met-Mb linearly increases with decrease of the pK_a of the axial H_2O. The correlation factor (0.86) is nearly unity when two outlying data points for Cu^{2+}-IDA1,2-Mb are omitted.[18] It was reported that the lowering of the pK_a reflects on the weakening of the hydrogen bond of the distal histidine (His 64) with the axial water.[19] The coordination environment of the iron site disordered by the weakened hydrogen bond might promote the rearrangement of the hexacoordinated met-Mb to the pentacoordinated deoxy-Mb during the electron-transfer reaction. This idea is consistent with the present result that the lower the pK_a of the axial H_2O is, the more accelerated the met-Mb reduction is. The redox potential of IDA*n*-Mb scarcely changed upon metal binding. The electron-transfer rate is controlled by several parameters, such as the reaction driving force, reorganization energy, and precomplexation property of Mb with ascorbate, according to the Marcus theory.[20] Reasonably, the present rate enhancement cannot be ascribed to the change of the driving force ($E_{1/2}$).[21] The structural data and the linear pK_a−reduction rate relationship strongly suggest that dynamic structural perturbations given upon the transition metal binding at the myoglobin surface which induce the lessened reorganization energy and/or the facilitated Mb−ascorbate complexation can effectively modulate the active site microenvironment. And as a result, the electron injection from ascorbate is accelerated in response to various metal cations in our engineered IDA*n*-Mbs.

In conclusion, we have established that the inserted iminodiacetic acid can play a crucial role as a reporter group in the metal responsive regulation of the Mb structure and the function. This is due to the transition metal triggered changes in the cofactor−apoprotein interactions. The present semisynthetic Mb is regarded as a prototype of the sophisticated biomaterials which can regulate the activity with sensing the concentration of the environmental metal ions. We envisage manipulation of activity of engineered biocatalysts through rationally designed artificial receptors.[22]

Experimental Section

Spectrophotometric Titration of IDA*n*-Mb with Metal Cations. A corresponding amount of metal salt ($CoCl_2$, $NiCl_2$, $CuSO_4$, $Zn(NO_3)_2$, $Cd(NO_3)_2$, or $MgSO_4$, 0−3 equiv) was added to an aqueous solution of IDA*n*-Mb (13.7 μM, 50 mM phosphate buffer (pH 8.0)) at 25 °C. After equilibrium (5−10 min later), the absorption spectra were measured.

Determination of pK_a of the Coordinated H_2O of IDA*n*-Mb. Spectrophotometric pH titrations for IDA*n*-Mbs in the presence of various metal cations were conducted by a conventional manners: IDA*n*-Mb, 13.7 μM, pH 6−11 (10 mM phosphate buffer) at 25 °C.

Reduction of IDA*n*-Mb by Ascorbate. To a solution of IDA*n*-Mb (13.7 μM, 50 mM phosphate buffer (pH 7.0)) was added an aqueous solution of ascorbic acid (final concentration, 0.2 mM), and the absorbance change at 580 nm was monitored by the time-scanning method at 25 °C. Separately, we confirmed quantitative conversion of met-Mb to oxy-Mb by the repeated scanning of UV−visible range (250−800 nm).

Measurement of the Redox Potential of IDA*n*-Mb. The redox potential of IDA*n*-Mb (Fe^{II}/Fe^{III}) was determined using a typical thin-layer spectroelectrochemical method.[23] Pt mesh was used as a working electrode, and methylene blue was a mediator: IDA*n*-Mb, 5.4 μM, 0.1 M KCl (50 mM phosphate buffer, pH 7.0) at 25 °C, optical cell length 1 mm under N_2 atmosphere, potentiostat, BAS 100W.

Syntheses. (a) *N*,*N*-Di(ethoxycarbonylmethyl)-*N*′-BOC-ethylenediamine (3). To a solution of *N*-BOC-ethylenediamine (500 mg, 3.1 mmol)[24] dissolved in 10 mL of dry DMF were added ethyl bromoacetate (3.3 mL, 31 mmol), KI (520 mg, 3.1 mmol), and $NaHCO_3$ (2.5 g, 30 mmol). After the mixed solution was stirred for 6 h at 25 °C, the residue was dissolved in 30 mL of $CHCl_3$ and washed with distilled water (30 mL × 2). The organic layer was dried over $MgSO_4$ and concentrated in vacuo. The title compound **3** was obtained as an oil (1.02 g, 96%). ^{1}H NMR ($CDCl_3$, 250 MHz): δ 1.29 (6H, t, $-CH_2CH_3$), 1.45 (9H, s, *t*-C_4H_9), 3.00 (2H, m, $-NHCH_2CH_2N=$), 3.27 (2H, m, $-NHCH_2CH_2N=$), 3.69 (4H, s, $-NCH_2CO-$), 4.20 (4H, q, $-CH_2CH_3$), IR (KBr, cm^{-1}): 3300 (ν_{NH}), 1730 (ν_{CO}).

(b) *N*,*N*-Di(ethoxycarbonylmethyl)ethylenediamine Ditrifluoroacetic Acid Salt (4). Into a solution of BOC derivative **3** (300 mg,

(17) Tamura, M.; Woodrow, G. V., III; Yonetani, T. *Biochim. Biophys. Acta* **1973**, *317*, 34.
(18) From Figure 4, we obtained the following equation: log $V_{init} = -0.96$ pK_a + 7.3, with a correlation factor of 0.86 where two data points for Cu^{2+} are omitted.
(19) (a) Tsukahara, K.; Yamamoto, Y. *J. Biochem.* **1982**, *93*, 15. (b) Tsukahara, K. *Inorg. Chem. Acta* **1986**, *124*, 199. (c) Tsukahara, K.; Okazawa, T.; Takahashi, H.; Yamamoto, Y. *Inorg. Chem.* **1986**, *25*, 4756.
(20) Marcus, R. A.; Sutin, N. *Biochim. Biophys. Acta* **1985**, *265*, 811.
(21) Since the transition metals are bound to the Mb surface, the facilitated electron transfer may be due to the electrostatic effect. To clarify this effect, we compared the rate of the reconstituted Mb with protohemin diethyl ester (pK_a = 8.0). The initial rate was determined to be one-half of the rate for Co^{2+}-bound IDA2-Mb, suggesting that the metal cation induced electrostatic effect may partially contribute to the rate acceleration.
(22) Noncovalent interactions of enzymes with some crown ethers have been reported: (a) Reinhoudt, D. N.; Egendebak, A. M.; Nigenhuis, W. F.; Verboom, W.; Kloosterman, M.; Schoemarker, H. E. *J. Chem. Soc., Chem. Commun.* **1996**, 2205. (b) Nagasaki, T.; Kimura, O.; Ukon, M.; Arimori, S.; Hamachi, I.; Shinkai, S. *J. Chem. Soc., Perkin Trans. 1* **1994**, 75. (c) Itoh, T.; Takagi, Y.; Murakami, T.; Hiyama, Y.; Tsukube, H. *J. Org. Chem.* **1996**, *61*. 2158.
(23) (a) Brunori, M.; Saggese, U.; Rotilio, G. C.; Antonini, E.; Wyman, J. *Biochemistry* **1971**, *10*, 1604. (b) Wilson, D. F.; Erecinska, M.; Ohnishi, T.; Dutton, P. L. *Bioelectrochem. Bioeng.* **1974**, *1*, 3. (c) Dickinson, L. C.; Chien, J. C. W. *J. Biol. Chem.* **1973**, *248*, 5005.
(24) Krapcho, A. P.; Kuell, C. S. *Synth. Commun.* **1990**, *20*, 2559.
(25) Brown, W. D.; Mebine, L. B. *J. Biol. Chem.* **1969**, *244*, 6696.

0.88 mmol) dissolved in 5 mL of dry CH_2Cl_2 (distilled over CaH_2) was added trifluoroacetic acid (TFA, 1.02 mL, 13.2 mmol) in 5 mL of dry CH_2Cl_2, dropwise over 30 min at 0 °C. After the mixed solution was stirred for 3 h at 25 °C, CH_2Cl_2 was evaporated off. The oily residue was dried in vacuo (50 °C, 0.06 Torr, 6 h). This is used in the next step without further purification. ^{1}H NMR ($CDCl_3$, 250 MH_z): δ 1.27 (6H, t, $-CH_2CH_3$), 3.27 (4H, m, $-NCH_2CH_2N-$), 3.74 (4H, s, $-NCH_2CO-$), 4.19 (4H, q, $-CH_2CH_3$), 7.69 (3H, bs, $-NH_3+$). IR (neat, cm^{-1}): 3300 (ν_{NH}), 1730 (ν_{CO}).

(c) 3,8,12,18-Tetramethyl-2,7-divinyl-13,17-bis[bis(ethoxycarbonylmethyl)aminoethylaminocarbamoylethyl]porphyrine (5). To the dry mixed solution (10 mL of THF and 10 mL of DMF) containing the preceding amine **4** (250 mg, 0.54 mmol) were added protoporphyrin IX (140 mg, 0.25 mmol), benzotriazole-1-yloxytris(dimethylamino)-phosphonium hexafluorophosphate (BOP, 240 mg, 0.55 mmol) and diisopropylethylamine (DIEA, 0.33 mL, 1.9 mmol). The reaction mixture was stirred for 1.5 h at 25 °C. After concentration, the residue was dissolved in 30 mL of $CHCl_3$ and washed with saturated $NaHCO_3$ (aq) (2 × 20 mL) and distilled water (1 × 20 mL). The organic layer was dried over $MgSO_4$ and concentrated in vacuo. The solid residue was further purified through chromatography (silica gel, column ∅ 3 cm × 20 cm, 5:1 $CHCl_3$:acetone and then 10:1 $CHCl_3$:methanol) to yield the product **5**, 170 mg (69%), as a dark-red solid, mp 155−158 °C. ^{1}H NMR ($CDCl_3$, 250 MHz): δ 0.97 (12H, t, $-CH_2CH_3$), 2.40 (4H, m, $-CH_2NCH_2CO-$), 3.02 (8H, m, $-CH_2CONHCH_2-$), 3.14 (8H, s, $-NCH_2CO-$), 3.56−3.68 (12H, m, Ar−CH_3), 3.82 (6H, q, $-CH_2CH_3$), 4.30 (4H, m, Ar−CH_2-), 6.18−6.45 (4H, dd, Ar−CH═CH_2), 7.79 (2H, s, −CONH−), 8.38−8.50 (2H, m, Ar−CH═CH_2), 10.10−10.17 (4H, m, meso-*H*). IR (KBr, cm^{-1}): 3300 (ν_{NH}), 1730 (ν_{CO}). Anal. Found: C, 65.28; H, 7.06; N, 11.17. Calcd for $C_{54}H_{70}N_8O_{10}$: C, 65.44; H, 7.12; N, 11.30. UV−visible spectrum ($CHCl_3$, nm): 407 (Soret), 505, 540, 575, 628.

(d) Iron(III) Complex 6 Derived from 5. The free base porphyrin derivative **5** (160 mg, 0.16 mmol) and $FeCl_2 \cdot 4H_2O$ (320 mg, 1.60 mmol) dissolved in 20 mL of dry DMF was heated at 65 °C for 6 h with stirring. DMF was evaporated off, and the black residue was dissolved in a mixed solvent ($CHCl_3$/THF (25 mL/5 mL)) and washed with 30 mL of HCl (aq) (pH 3.0) until the yellow color due to $FeCl_2$ in aqueous solution disappeared. The organic layer was dried over $MgSO_4$ and concentrated in vacuo. The title compound **6** was obtained as a dark-red solid (110 mg, 63%), mp 164−166 °C. IR (KBr, cm^{-1}): 3300 (ν_{NH}), 1730 (ν_{CO}). UV−visible spectrum (10:1 $CHCl_3$:methanol, nm): 396 (Soret), 504, 634.

(e) IDA2-Heme 2 Derived from 6. To a mixed solution (8 mL, 1:2 THF:MeOH) of **6** (50 mg, 0.046 mmol), 550 μL of 1 N NaOH (aq) was added. After 30 min of stirring, a few drops of distilled water was added in order to dissolve the formed precipitate. After 1 day of stirring 20 mL of distilled water was added and the solution was acidified to pH 3.0 with 1 N HCl (aq). The resulting precipitate was collected by centrifuge (10 000 rpm, 5 min) and washed with distilled water. The dark-red solid was purified through gel chromatography (Sephadex LH-20; eluent, DMF) to obtain the product **2** (25 mg, 58%), mp >300 °C. Anal. Found: C, 56.67; H, 5.46; N, 11.49. Calcd for $C_{46}H_{52}N_8O_{10}ClFe \cdot 0.4H_2O$: C, 56.64; H, 5.46; N, 11.49. IR (KBr, cm^{-1}): 3300 (ν_{NH}), 1710 (ν_{CO}). UV−visible spectrum (DMF, nm): 387 (Soret), 509, 636.

(f) 3,8,12,18-Tetramethyl-2,7-divinyl-13-(ethoxycarbonylethyl)-17-[bis(ethoxycarbonylmethyl)aminoethylaminocarbamoylethyl]-porphyrine (7). Protoporphyrin IX (PPIX) monoethyl ester (224 mg, 0.96 mmol) was converted to the title compound (100 mg, 26%) as described in previous text, mp 186−188 °C. ^{1}H NMR ($CDCl_3$, 250 MHz): δ 0.95 (6H, t, $-CH_2CH_3$), 1.05 (6H, t, $-CH_2CH_3$), 2.34 (2H, m, $-CH_2NCH_2CO-$), 2.98 (6H, m, $-CH_2CONHCH_2-$, $-CH_2COCH_2-CH_3$), 3.10 (4H, s, $-NCH_2CO-$), 3.5−3.7 (12H, m, Ar−CH_3), 3.78 (4H, q, $-CH_2CH_3$), 4.05 (2H, q, $-CH_2CH_3$), 4.30 (4H, m, Ar−CH_2-), 6.1−6.5 (4H, dd, Ar−CH═CH_2), 7.65 (1H, m, −CONH−), 8.4−8.5 (2H, m, Ar−CH═CH_2), 10.1−10.2 (4H, m, meso-*H*). IR (KBr, cm^{-1}): 3300 (ν_{NH}), 1730 (ν_{CO}). UV−visible spectrum ($CHCl_3$, nm): 407 (Soret), 505, 540, 575, 628.

(g) Iron(III) Complex 8 Derived from 7. Compound **7** (70 mg, 0.087 mmol) was converted to the title compound (55 mg, 71%) as described in previous text, mp 135−137 °C. IR (KBr, cm^{-1}): 3300 (ν_{NH}), 1730 (ν_{CO}). UV−visible spectrum (10:1 $CHCl_3$:methanol, nm): 388 (Soret), 509, 635.

(h) IDA1-Heme 1 Derived from 8. Iron(III) Complex **8** (35 mg, 0.039 mmol) was converted to the title compound (26 mg, 81%) as described in previous text, mp > 300 °C. Anal. Found: C, 58.84; H, 5.35; N, 9.97. Calcd for $C_{40}H_{42}N_6O_7ClFe \cdot 0.5H_2O$: C, 58.65; H, 5.29; N, 10.26. IR (KBr, cm^{-1}): 3300 (ν_{NH}), 1710 (ν_{CO}). UV−visible spectrum (DMF, nm): 387 (Soret), 509, 635.

IC961474V